JOURNAL OF BACTERIOLOGY, Apr. 2008, p. 2920–2932 Vol. 190, No. 8
0021-9193/08/$08.00+0 doi:10.1128/JB.01868-07

Identification of a Second Lipopolysaccharide in *Porphyromonas gingivalis* W50▽

Minnie Rangarajan,[1]* Joseph Aduse-Opoku,[1] Nikolay Paramonov,[1] Ahmed Hashim,[1] Nagihan Bostanci,[2] Owen P. Fraser,[3] Edward Tarelli,[3] and Michael A. Curtis[1]

Centre for Infectious Disease, Institute of Cell and Molecular Science,[1] and Centre for Clinical and Diagnostic Oral Sciences,[2] Barts and The London Queen Mary's School of Medicine and Dentistry, 4 Newark Street, London E1 2AT, United Kingdom, and Medical Biomics Centre, St. George's University of London, Cranmer Terrace, London SW17 0RE, United Kingdom[3]

Received 28 November 2007/Accepted 28 January 2008

We previously described a cell surface anionic polysaccharide (APS) in *Porphyromonas gingivalis* that is required for cell integrity and serum resistance. APS is a phosphorylated branched mannan that shares a common epitope with posttranslational additions to some of the Arg-gingipains. This study aimed to determine the mechanism of anchoring of APS to the surface of *P. gingivalis*. APS was purified on concanavalin A affinity columns to minimize the loss of the anchoring system that occurred during chemical extraction. ^{1}H nuclear magnetic resonance spectroscopy of the lectin-purified APS confirmed the previous structure but also revealed additional signals that suggested the presence of a lipid A. This was confirmed by fatty acid analysis of the APS and matrix-assisted laser desorption ionization–time of flight mass spectrometry of the lipid A released by treatment with sodium acetate buffer (pH 4.5). Hence, *P. gingivalis* synthesizes two distinct lipopolysaccharide (LPS) macromolecules containing different glycan repeating units: O-LPS (with O-antigen tetrasaccharide repeating units) and A-LPS (with APS repeating units). Nonphosphorylated penta-acylated and nonphosphorylated tetra-acylated species were detected in lipid A from *P. gingivalis* total LPS and in lipid A from A-LPS. These lipid A species were unique to lipid A derived from A-LPS. Biological assays demonstrated a reduced proinflammatory activity of A-LPS compared to that of total LPS. Inactivation of a putative O-antigen ligase (*waaL*) at PG1051, which is required for the final step of LPS biosynthesis, abolished the linkage of both the O antigen and APS to the lipid A core of O-LPS and A-LPS, respectively, suggesting that WaaL in *P. gingivalis* has dual specificity for both O-antigen and APS repeating units.

The gram-negative anaerobic bacterium *Porphyromonas gingivalis* is an important etiological agent in periodontal disease and produces several virulence factors. Among them are the cysteine proteases Arg-gingipain (Rgp) and Lys-gingipain (Kgp), which are capable of causing the degradation of several host proteins and lipopolysaccharide (LPS), which may exacerbate the inflammatory response in periodontal tissues of the infected host (2, 9) These factors are also important antigens in patients with periodontal disease and may account for a significant proportion of the immune response directed against *P. gingivalis* (27, 38). A monoclonal antibody (MAb), 1B5, raised against one of the five isoforms of Arg-gingipains (Rgps), $RgpA_{cat}$, also cross-reacts with two other Rgps, namely, mt-$RgpA_{cat}$ and mt-RgpB, and also cross-reacts with an anionic cell surface polysaccharide (APS) (10, 30). Chemical deglycosylation of $RgpA_{cat}$ and mt-$RgpA_{cat}$ with anhydrous trifluoromethane sulfonic acid abolishes their cross-reactivity to MAb 1B5, indicating that this antibody recognizes a carbohydrate epitope that is also present in APS (10, 30).

We established that APS was distinct from LPS and capsular polysaccharide (PS) (K antigen) in *P. gingivalis* (30). LPS purified by a procedure described previously by Darveau and Hancock (11) did not show immunoreactivity to MAb 1B5, indicating that APS and LPS are two different PSs present in *P. gingivalis* W50. In addition, the O antigens prepared from the LPS of *P. gingivalis* W50 and LPS from a mutant strain (*porR*) (PG1138), which lacks cross-reactivity with MAb 1B5 (36), showed the same structure for the repeating unit (30). Since natural capsule-minus isolates and a mutant strain of *P. gingivalis* W50 defective in capsule biosynthesis all reacted with MAb 1B5, we also concluded that APS is unrelated to the K antigen of *P. gingivalis* (3, 30).

We described the structural analysis of APS (30) by nuclear magnetic resonance (NMR) spectroscopy and methylation analysis and showed it to be a phosphorylated branched mannan. The backbone is composed of α-1,6-linked Man residues, and the side chains contain α-1,2-linked Man oligosaccharides (OSs) of different lengths (one or two Man residues) attached to the backbone via an α-1,2 linkage. One of the side chains in the repeating unit contains Manα1-2Manα-1-phosphate linked via phosphorus to a backbone Man at position 2. De-*O*-phosphorylation of APS abolished cross-reactivity but did not cause the depolymerization of APS, suggesting that the Manα1-2Manα1-phosphate fragment forms part of the epitope recognized by MAb 1B5. Thus, APS represents a novel PS that is immunologically related to the posttranslational additions to the Arg-gingipains $RgpA_{cat}$, mt-$RgpA_{cat}$, and mt-RgpB.

Mutant strains defective in APS biosynthesis are significantly more sensitive to serum killing than the parent strain (37).

* Corresponding author. Mailing address: Centre for Infectious Disease, Institute of Cell and Molecular Science, Barts and The London Queen Mary's School of Medicine and Dentistry, 4 Newark Street, London E1 2AT, United Kingdom. Phone: 0207 882 2320. Fax: 0207 882 2181. E-mail: m.rangarajan@qmul.ac.uk.

▽ Published ahead of print on 8 February 2008.

TABLE 1. Sequences of oligonucleotides used in this study

Primer	Gene targeted	Sequence (5′→3′)[c]	Size of amplicon (bp)	Description or reference
PG1051F1[a]	PG1051	ACGTTTTCGGTTCGGTTCG		Allelic exchange
PG1051R1 (SstI)	PG1051	atatat**gagctc**ATTCCGTTCTTGTCGGACG	505	
PG1051F2[a] (XbaI)	PG1051	atatat**tctaga**ATCTTCAACGGCCTCTTGTC		Allelic exchange
PG1051R2	PG1051	TTTCGAGTCGGAGAAACGG	385	
PG1050F1[b] (NotI)	PG1051	atatat**gcggccgc**CGTTTGCGTTGCAGTACGG		
PG1052R1 (NotI)	PG1051	atatat**gcggccgc**GGATGAGCCGCACCATTTC	2,161	Complementation
RTPG1050F1	PG1050	CACGAGGCATACGAGCATG	562	Expression
RTPG1050R1	PG1050	TCCGAAGAGCATGTCCCTC		
RTPG1051F1	PG1051	TTGTTGTTGCTGCGGTAGG	1,062	Expression
RTPG1051R1	PG1051	TTCGACTGCCATTGTCAGG		
RTPG1052F1	PG1052	GTTCGATCTGCCGGATTCC	209	Expression
RTPG1052R1	PG1052	CATTGGTCGATGGCATCAC		
ErmFR2	*ermF*	TTCGTTTTACGGGTCAGCAC		
ErmAMR2	*ermAM*	ACTTTGGCGTGTTTCATTGC		3

[a] Ligation of these amplicons to the *erm* cassette leads to a deletion of 464 bp within the 1,416 bp of PG1051.
[b] Incorporates PG1051 and flanked partly by regions of PG1050 and PG1052.
[c] Lowercase type indicates irrelevant sequences to facilitate restriction digestion following DNA amplification, and boldface type corresponds to restriction sites.

Furthermore, cells of the *porR* mutant of *P. gingivalis*, which lack APS, were shown to be more fragile and prone to lysis than the parent W50 strain (30, 36). Although the growth profiles of *P. gingivalis* W50 and *porR* mutant strains in complex medium are almost identical up to early stationary phase, *porR* cells lyse rapidly thereafter, leading to a steep decline in the culture optical density. Electron micrographs of cells of *P. gingivalis* W50 and *porR* mutant strains grown in liquid cultures for 48 h demonstrated a significant reduction in the electron-dense surface layer in cells from the *porR* mutant strain (30). Together, these data suggest that APS forms an important constituent of the bacterial surface and is required for optimal cell integrity and serum resistance.

Although the structure and localization of APS were known from those previous studies (30), the mechanism of anchoring of APS to the surface of *P. gingivalis* was unknown. However, there are a number of possibilities. First, there may not be a specific structural entity responsible for anchoring APS to the cell surface. Second, there may be an anchoring moiety, but it may form such a minor component of the purified APS that it was not detectable in our initial studies (30). Third, the structural entity may have been lost or destroyed by the methods employed for the purification of APS; some of the column chromatography steps employed for APS purification were carried out in the presence of sodium deoxycholate in buffers at pH 9.5 (30). Although the presence of sodium deoxycholate helps to solubilize APS, thereby enabling ease of purification, the high pH of the buffers employed may have caused the hydrolysis of APS from a labile anchoring molecule on the cell surface of *P. gingivalis*.

In the present study, we aimed to use our knowledge of the structure of APS to develop an extraction-and-purification procedure employing less harsh conditions than the original methods. The aim was to determine whether there is a labile anchoring component in this macromolecule responsible for tethering APS to the cell surface of *P. gingivalis*. Having identified a putative anchor, we also used a genetic approach to confirm this finding.

MATERIALS AND METHODS

Materials. Concanavalin A (ConA)-Sepharose 4B, Sephacryl S-200HR, DEAE-Sephacel, and PlusOne urea were purchased from GE Healthcare, Amersham Place, Buckinghamshire, United Kingdom. All other chemicals were obtained from VWR, Lutterworth, Leicestershire, United Kingdom, or from Sigma-Aldrich Company Ltd., Poole, Dorset, United Kingdom, and were the purest grades available. A solution containing 30% acrylamide–Bis (37.5:1) was obtained from Bio-Rad Laboratories (Hercules, CA). Horseradish peroxidase-labeled mouse immunoglobulin was purchased from Dako A/S, High Wycombe, Buckinghamshire, United Kingdom. Restriction and modification enzymes were purchased from New England Biolabs, and DNA purification reagents were obtained from Qiagen. RNA isolation and analysis reagents were obtained from ABgene.

Bacterial growth conditions. *P. gingivalis* W50 was grown on either blood agar plates containing 5% defibrinated horse blood or brain heart infusion (BHI) broth supplemented with hemin (5 mg ml^{-1}) in an anaerobic atmosphere of 80% N_2, 10% H_2, and 10% CO_2 (2). The cells were harvested, washed with phosphate-buffered saline, and freeze-dried for the isolation of APS. Clindamycin HCl and tetracycline HCl were added at 5 μg ml^{-1} and 1 μg ml^{-1}, respectively, for the selection of *ermF* and *tetQ* in *P. gingivalis*. Ampicillin (Na^+ salt, 100 μg ml^{-1}) or erythromycin (300 μg ml^{-1}) was added to the growth medium to select for pUC-derived or *ermAM*-containing plasmids in *Escherichia coli*, respectively. *E. coli* XL1-Blue (Stratagene) was used for cloning.

Inactivation of a putative O-antigen ligase, PG1051. A putative O-antigen ligase, PG1051, was identified from the *P. gingivalis* genome based on topology, which was comparable to that of *E. coli* WaaL. A mutant with a defect in PG1051 was generated by allelic exchange mutagenesis. Primer pairs F1 and R1 and F2 and R2, incorporating restriction sites, were designed to amplify the 5′ (SstI) and 3′ (XbaI) ends of PG1051 (Table 1). They were then ligated into the SstI-XbaI fragment of the *erm* cassette (15) and reamplified. The *erm* cassette fragment consists of tandem *ermF* and *ermAM* genes encoding macrolide-lincosamide resistance; *ermF* is expressed in *Bacteroides-Porphyromonas*, and *ermAM* is expressed in *E. coli*. Following blunting with End^{IT} (Ambion), the new amplicon containing the *erm* cassette flanked by PG1051 sequences was cloned into the SmaI site of pUC18not (18) and transformed into competent cells of *E. coli* XL1-Blue. Recombinant plasmid pSN1, restricted with NotI, was used to transform exponential cells of *P. gingivalis* as described previously (3). Twelve clin-

damycin-resistant colonies were picked at random and screened by observing their pigmentation and hemolysis on blood agar plates followed by PCR and growth rates in BHI broth. The results were identical in all the isolates. One representative, PG1051(G), was used in all subsequent experiments and is referred to as PG1051-KO.

Complementation of PG1051-KO. PG1050 and PG1051 are separated by 41 bp, and PG1051 and PG1052 are separated by 64 bp, and they could constitute an operon. Therefore, to complement inactivated PG1051-KO in *P. gingivalis*, the gene was cloned into the NotI site of pUCET1 (7) to include 500-bp upstream sequences using primer sets 1050F1 and 1052R1 (Table 1 and see Fig. 6A). The resulting plasmid, pBL5 (linearized with BamHI), with all the genes in the same orientation, was used to transform exponential cells of *P. gingivalis* PG1051-KO essentially as described above. The complemented region is shown in Fig. 6B. The correct integration of plasmid was checked using primer pair ermFF2 and ermAMR2 in PCRs (results not shown) (3). Six complemented strains were selected at random and screened as described above, and a representative strain, PG1051$^+$(G), was selected for all subsequent analyses and is referred to as PG1051$^+$.

Reverse transcription-PCR. The genes targeted and the primer sets used are listed in Table 1. Reverse transcription was carried out in Reddy Load Reverse iT One Step PCR master mix (ABgene) using the following parameters: 55°C (30 min) for first-strand cDNA synthesis followed by the inactivation of the enzyme and 35 cycles of 94°C (30 s), 60°C (30 s), and 72°C (1 min). A final extension step was applied at 72°C (5 min).

Isolation of APS. PS/LPS was extracted from freeze-dried *P. gingivalis* W50 cells (0.5 to 0.75 g) using a modified phenol-water procedure (40), followed by exhaustive dialysis against distilled water. The water-insoluble material was removed by centrifugation at 10,000 × *g*, and the supernatant was freeze-dried.

The freeze-dried residue (75 mg) was dissolved in 15 ml of a solution containing 50 mM Tris-HCl–10 mM $MgCl_2$ (pH 7.5) and treated with DNase I, RNase A, and proteinase K at 37°C, as described previously (30). The reaction mixture was dialyzed against distilled water and freeze-dried.

Affinity chromatography on ConA-Sepharose 4B. The freeze-dried crude material (42 mg) was dissolved in 25 ml of a solution containing 20 mM Tris-HCl–0.5 M NaCl–2 mM $MnCl_2$–2 mM $CaCl_2$ (pH 7.4), placed into an ultrasonic bath at 25°C for 1 h, and applied to a column of ConA-Sepharose 4B (2.6 cm by 10 cm) equilibrated in the same buffer at 22°C. The column was washed with buffer until the A_{280} was ~0.05, and any bound material was eluted with 0.25 M α-methyl-manno-pyranoside in 20 mM Tris-HCl–0.5 M NaCl (pH 7.4). Fractions (2 ml) were collected. Usually, the flow was stopped after 0.5 column volumes of eluent had gone through, and the column was transferred to 4°C overnight. Elution was resumed the following day after the column had been allowed to equilibrate to room temperature. Usually, 6 to 8 column volumes of eluent were sufficient to elute all APS from the affinity column.

Aliquots (10 μl) of column fractions were subjected to sodium dodecyl sulfate (SDS)-polyacrylamide gel electrophoresis (PAGE) and Western blotting with MAb 1B5 as described previously (30). Fractions that showed immunoreactivity with MAb 1B5 were combined, dialyzed against distilled water at 4°C, and freeze-dried.

Ion-exchange chromatography. The freeze-dried residue from the affinity column was dissolved in 20 ml of 50 mM ammonium bicarbonate (pH 8.1) and applied to a column of DEAE-Sephacel (1.6-cm internal diameter by 4 cm) equilibrated in the same buffer at 22°C. The refractive index of column effluent was monitored (Knauer Wellchrom K-2400 RI detector; Wissenschaftliche Geratebau, Ing., Herbert Knauer GmbH, Berlin, Germany) until there was no change in the refractive index of the column effluent. Negatively charged APS was eluted with a gradient of 0 to 1 M NaCl in buffer (total volume, 80 ml), followed by a gradient of 1 M to 2 M NaCl (total volume, 80 ml) at a flow rate of 60 ml/h. The A_{280} of column fractions (2.5 ml) was measured, and aliquots (10 μl) were subjected to SDS-PAGE and Western blotting with MAb 1B5. The neutral PS was not cross-reactive with MAb 1B5, whereas acidic fractions showed cross-reactivity. The immunoreactive fractions were combined, dialyzed against distilled water, and freeze-dried.

Final purification of APS. The freeze-dried residue of crude APS was subjected to a final gel filtration step on Sephacryl S-200HR columns (1.6-cm internal diameter by 67 cm) equilibrated in 50 mM ammonium bicarbonate (pH 8.1) at 22°C. This step yielded 3 mg of pure APS, which was cross-reactive with MAb 1B5 and used for further analysis.

Isolation of LPS. LPS was prepared using an LPS extraction kit from Intron Biotechnology (South Korea) and was used in SDS-urea-PAGE experiments (19). For the analysis of lipid A from *P. gingivalis* W50 and *porR* mutant strains by matrix-assisted laser desorption ionization (MALDI)–time of flight (ToF) mass spectrometry (MS), LPS was isolated from freeze-dried whole bacterial cells (10 mg) using TRIzol (Invitrogen) as described previously by Yi and Hackett (44). Lipid A was isolated from crude LPS and LPS with APS repeating units (A-LPS) by mild acid hydrolysis in 10 mM sodium acetate (pH 4.5) containing 1% SDS (44) and used in biological assays.

SDS-PAGE and Western blotting. SDS-PAGE of the various column fractions was performed according to methods described previously by Laemmli (23), using 12.5% (wt/vol) acrylamide gels. Samples were transferred onto nitrocellulose membranes and probed with MAb 1B5 as described previously (30). LPS preparations (10 to 20 μg) from *P. gingivalis* W50 and mutant strains were subjected to SDS-urea-PAGE in polyacrylamide slab gels at 10°C for 3 to 4 h using procedures described previously by Inzana and Apicella (19). Gels were stained with silver.

MALDI-ToF MS. MALDI-ToF MS was performed using a Kratos Axima curved field reflection instrument (Kratos Analytical Ltd., Manchester, United Kingdom) fitted with a nitrogen laser operating at 337 nm using pulsed extraction in negative linear mode. Lipid A was analyzed using Norharmane (9H-pyrido[3,4]indole) in methanol at a concentration of 10 mg/ml used as a matrix. A total of 0.5 μl of lipid A solution in water (~100 pmol/μl), together with 0.5 μl of matrix solution, was applied to the MALDI plate and allowed to dry in air. The instrument was calibrated using the peptides Des-Arg1 Bradykinin (mass, 904.0), angiotensin 1 (mass, 1,296.5), and neurotensin (mass, 1,672.3), and average masses were used throughout.

NMR spectroscopy. ^{1}H and ^{31}P one-dimensional NMR spectra were obtained on a Bruker AV600 spectrometer using Xwinnmr v.3.5 Bruker software. ^{1}H NMR spectra were acquired at 40°C using acetone as an internal standard (δ_H 2.225). ^{31}P NMR spectra were run at 40°C. Chemical shifts for phosphorus spectra are given relative to 85% orthophosphoric acid (δ_P 0.00).

Monosaccharide analysis. The monosaccharide composition of APS was determined by methanolysis as described previously (5). Methyl glycosides were converted to *O*-trimethylsilyl (O-TMS) ethers and analyzed by gas chromatography (GC)-MS (20) (Agilent Technologies Ltd., Cheshire, United Kingdom).

Analysis of fatty acids. APS was treated with methanolic HCl (3 M) at 85°C for 5 h. After removal of methanolic HCl, the reaction mixture was re-N-acetylated (5), and methyl glycosides of sugars and methyl esters of fatty acids released were converted to O-TMS ethers and analyzed by GC-MS as described above.

Transmission electron microscopy. *P. gingivalis* cells were grown for 24 h in BHI broth containing hemin and fixed in glutaraldehyde. Transmission electron microscopy was performed in Na-cacodylate buffer as described previously (37), using a Jeol JEM 1230 electron microscope equipped with a Morada digital camera.

Stimulation of the myelomonocytic cell line MonoMac-6. The myelomonocytic cell line MonoMac-6 was obtained from the German Collection of Microorganisms and Cell Cultures (Mascheroder, Braunschweig, Germany). MonoMac-6 cells were cultured in RPMI-Glutamax (Invitrogen Ltd., Paisley, United Kingdom) supplemented with 10% fetal bovine serum, 1% nonessential amino acids (Invitrogen Ltd.), 1% sodium pyruvate (Invitrogen Ltd.), and 9 μg/ml bovine insulin (Sigma-Aldrich, Poole, Dorset, United Kingdom). MonoMac-6 cells (1×10^6 cells/ml) were used for cytokine induction assays in six-well dishes in the absence or presence of microbial stimulants. Experiments were carried out in triplicate. In order to assay total cytokines (cell-associated and secreted), cells were lysed by three freeze-thaw cycles. Cell-free culture supernatants were collected by centrifugation at 1,000 rpm for 5 min and stored at −80°C till required.

Measurement of cytokine production. Cytokine production (interleukin-1α [IL-1α], IL-1β, IL-6, and IL-8) in cell-free culture supernatant was measured using commercially available specific enzyme-linked immunosorbent assay (ELISA) kits (R&D Systems, Minneapolis, MN). The absorbance at 450 nm was measured using a microplate reader with a wavelength correction set at 570 nm to subtract background. A standard curve was generated using a four-parameter logistic curve fit (Excel) for each set of samples assayed.

Determination of endotoxin levels in lipid A preparations. Bacterial endotoxin was assessed using a chromogenic limulus amebocyte lysate test (QCL1000; Cambrex Bio Science, United Kingdom). Lipid A from *P. gingivalis* total LPS and A-LPS was dissolved in pyrogen-free water, and serial dilutions were made. The absorbance of the samples at 405 nm was measured, and the endotoxin concentration was calculated from a standard curve using *E. coli* endotoxin as a reference standard. The detection limit of the assay was 0.1 endotoxin units (EU)/ml.

Cell viability assays. Cell viability was determined by measuring lactate dehydrogenase (LDH) release using the CytoTox 96 nonradioactive cytotoxicity assay (Promega UK, Southampton, United Kingdom). MonoMac-6 cells were exposed to *P. gingivalis* total lipid A or lipid A from A-LPS (0.06 to 2.5 EU/ml) and incubated for 6 h at 37°C. Fifty microliters of supernatant per well was carefully removed and transferred onto an optically clear 96-well plate. Reaction solution was added to each well and incubated for 30 min in the dark. The reaction was

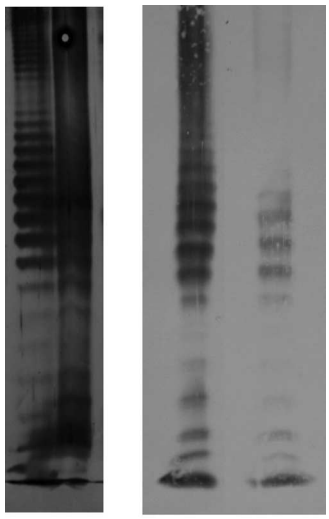

FIG. 1. SDS-PAGE and Western blotting of *P. gingivalis* W50 total LPS and pure A-LPS. (A) SDS-urea-PAGE. (B) Western blotting versus MAb 1B5 of *P. gingivalis* W50 total LPS prepared using the phenol-guanidine isothiocyanate method and A-LPS purified by ConA affinity chromatography. Lanes: 1 and 3, W50 total LPS; 2 and 4, pure A-LPS.

stopped by the addition of 1 M HCl to the mixture, and the absorbance at 490 nm was measured using an ELISA plate reader (model 680; Bio-Rad Laboratories, Hemel Hempstead, United Kingdom). The enzyme activity released from damaged cells into the supernatant was expressed as a percentage of total LDH activity released from cells lysed by exposure to 0.1% Triton X-100 for 45 min. Values represent the means ± standard deviations of three wells.

Statistical analysis. A Student's *t* test for paired values was used, and data were considered to be significant at a *P* value of <0.05.

RESULTS

Isolation of APS. Since the APS contained a branched mannan as the repeating unit, ConA-lectin-Sepharose 4B was used as the affinity matrix to selectively bind APS. However, APS has only a moderate binding affinity for this lectin since higher concentrations of α-methyl-mannopyranoside (1 M) or 0.1 M borate buffer (pH 6.5) did not elute any additional MAb 1B5-reactive material from the column. All the APS present in the phenol extract did not bind to the ConA affinity column, probably due to the reduced solubility of APS in binding buffer caused by the size of the molecule or due to steric reasons. One of the main differences between APS purified by lectin affinity chromatography and APS obtained by conventional purification methods in the presence of sodium deoxycholate in buffers at pH 9.5 (30) was its solubility, especially at pHs below 8.1. Since ConA is active at pH 7.4 and requires the presence of Mn^{2+} and Ca^{2+} to maintain its tetrameric structure, it is possible that APS may precipitate on the column under these conditions.

Figure 1 shows the SDS-urea-PAGE profile of APS followed by silver staining and Western blotting with MAb 1B5. *P. gingivalis* W50 total LPS is also shown for comparison. APS shows the characteristic laddering pattern of LPS, and it is interesting that W50 total LPS shows bands in the entire region of the resolving gel by both silver staining and Western blotting, whereas APS shows bands only in the intermediate- and low-molecular-weight regions. This suggests that affinity chromatography on ConA-Sepharose selectively binds intermediate- to low-molecular-weight species of APS, probably due to solubility, as described above.

NMR spectroscopy. The ^{1}H NMR spectrum of APS showed proton resonances in the anomeric region at 4.90 to 5.5 ppm similar to those from previously reported spectra (30) (Fig. 2A and B and Table 2). The positions of H-2 for the terminal, 2-substituted, and 2,6-disubstituted mannose residues were in accordance with those assigned for the branched mannan containing monophosphate in the diester linkage. Hence, these findings confirmed the structure of APS as a branched phosphorylated mannan as previously described (30).

A number of signals in the region at 0.8 to 1.6 ppm (Table 2) could be assigned to fatty acid residues of a lipid A moiety (32), and signals at 2.68 ppm and 2.53 ppm could be assigned to the H-2 of 3-OH fatty acids. Finally, the presence of H-3ax of a 2-keto-3-deoxyoctulosonic acid residue at 2.047 ppm led us to conclude that this ConA-purified APS may contain a lipid A and that the minor proton signals that could not be assigned may represent components of an OS core associated with this lipid A. Monosaccharide analysis of APS by methanolysis followed by re-N-acetylation and GC-MS of O-TMS ethers of the methylglycosides resulted in the detection of Man (80%), Glc (7%), Gal (7%), GlcNAc (3.5%), and Rha (1.1%) (Fig. 3).

Fatty acid analysis of pure APS using methanolysis (3 M methanolic HCl) and the same derivatization procedure showed the presence of 3-OH $C_{17:0}$ and lower amounts of 3-OH $C_{15:0}$ and $C_{16:0}$ fatty acids (not shown). These low levels could be due to the inability of methanolic HCl (3 M) to release O-linked fatty acids in high yields. The monosaccharide composition is in accordance with an overall macromolecular structure in which the branched phosphorylated mannan represents the major component of APS, while the other sugars present in much smaller relative amounts could correspond to a core OS. Importantly, GalNAc, which is a constituent of the tetrasaccharide repeating unit of the O antigen of *P. gingivalis* LPS (29), was not detected in these analyses, suggesting that the lipid A and core OS present in lectin-purified APS are not derived from contaminating LPS in this preparation.

For ease of presentation, we therefore refer to this lectin-purified polysaccharide as A-LPS, in which we propose that the phosphorylated branched mannan repeating unit (APS) is linked to a lipid A core. Conversely, LPS containing the tetrasaccharide repeating unit (O antigen), previously described by Paramonov et al. (29), linked to a lipid A core is referred to as O-LPS.

Analysis of lipid A from O-LPS and A-LPS. Lipid A was isolated from pure A-LPS by treatment with 1% SDS in 10 mM sodium acetate at 100°C (44) and analyzed by MALDI-ToF MS (Fig. 4A).

Four main clusters of peaks were detected at approximately *m/z* 1,376, *m/z* 1,449, *m/z* 1,593, and *m/z* 1,657 (Fig. 4A). The clusters around *m/z* 1,657 and *m/z* 1,449 in the MS of lipid A from A-LPS could be assigned to monophosphorylated penta-acylated and monophosphorylated tetra-acylated lipid A species, respectively. The cluster of peaks around *m/z* 1,593 cor-

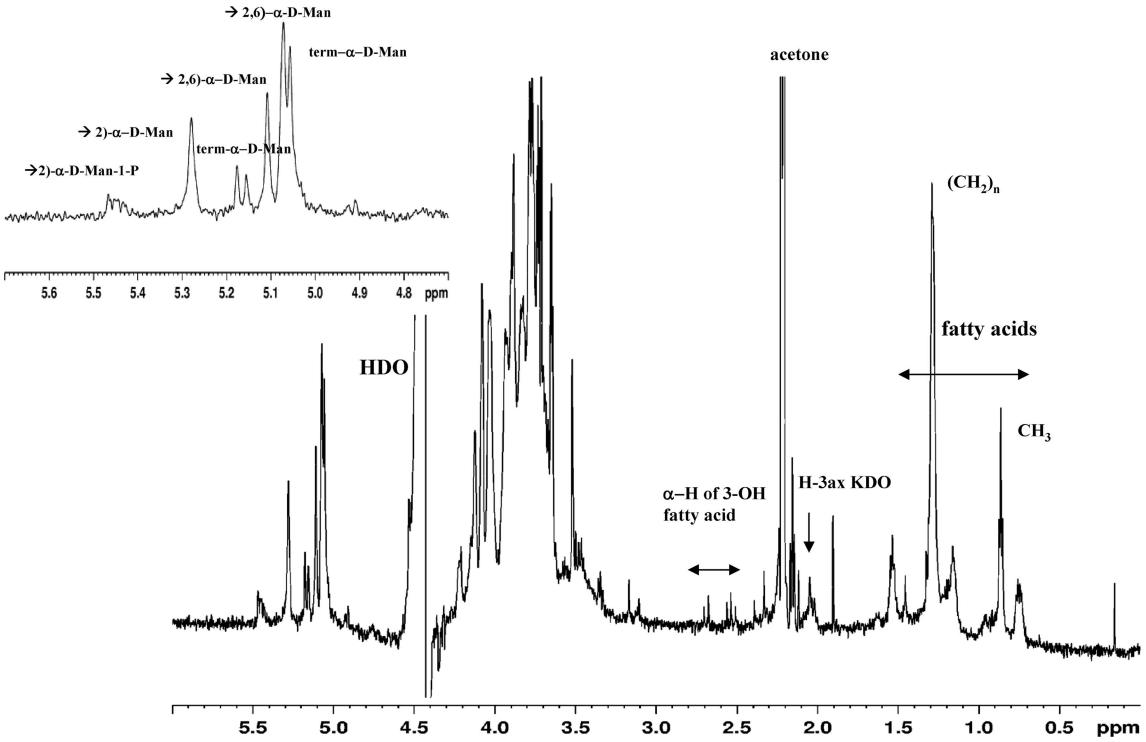

FIG. 2. One-dimensional ^{1}H NMR spectrum of APS acquired in D_2O at 40°C. The signals for CH_3 and $(CH_2)_n$ groups of fatty acids, H-2 of 3-OH fatty acids of lipid A, and H-3ax of 2-keto-3-deoxyoctulosonic acid (KDO) from the core region are indicated. The inset shows the anomeric region, and the signals of the protons refer to 2-linked, 2,6-linked, and terminal α-D-mannopyranosyl residues as indicated.

responds to nonphosphorylated penta-acylated lipid A, and signals at *m/z* 1,376 represent nonphosphorylated tetra-acylated lipid A species. Heterogeneity within these clusters probably reflects differences in fatty acid chain lengths (14 mass units), a phenomenon previously ascribed to the relaxed specificity of the fatty acyl chain transferase activity of *P. gingivalis* (4). The experiment was performed with two independently purified samples of APS, and the results were reproducible. A portion of pure A-LPS was also analyzed by MALDI-ToF MS without prior treatment with sodium acetate at 100°C. No signals due to lipid A species were detected (data not shown). This suggests that lipid A detected in A-LPS is covalently linked to APS, probably via a core OS.

TABLE 2. ^{1}H NMR data for APS (A-LPS)[a]

Proton	Mannose residue[b]	N/O-linked 3 OH fatty acid[c]
H-1; H-2	5.45; 4.04 →2)-α-Man-P	
H-1; H-2	5.28; 4.12 →2)-α-Man	
H-1; H-2	5.18; 4.08 term-α-Man	
H-1; H-2	5.16; 4.08 term-α-Man	
H-1; H-2	5.12; 4.03 →2,6)-α-Man	
H-1; H-2	5.10; 4.04 →2,6)-α-Man	
H-1; H-2	5.07; 4.12 →2,6)-α-Man	
H-1; H-2	5.06; 4.08 term-α-Man	
$-CHMe_2$ (m)		1.54
$(CH_2)_n$ (m)		1.29
α-CH_2 (m)[d]		1.16
ω-CH_3 (t) $J_{1,2}$ 7.04 Hz		0.86

[a] δ_H in ppm.
[b] Data for the linkage of α-mannose residues were described previously by Paramonov et al. (30).
[c] Data for the linkage of N/O-linked 3-OH fatty acids were described previously by Que-Gewirth et al. (32).
[d] The position of this methylene group refers to an *O*-acyloxy substituent at position 3 in some of the O/N-linked fatty acids.

We were unable to prepare O-LPS free from contaminating A-LPS except using procedures that compromise lipid A structure, such as the cold $MgCl_2$-ethanol procedure described previously by Darveau and Hancock (11). We were therefore unable to perform a direct comparison of the lipid A components of A-LPS and O-LPS. As an alternative, we compared the total lipid A composition of *P. gingivalis* W50 (containing both A-LPS and O-LPS) with that from a *P. gingivalis porR* mutant strain that produces only O-LPS. Figures 4B and C show the mass spectra obtained for *P. gingivalis* W50 lipid A and *porR* mutant strain lipid A, respectively. The analyses were performed on two independently isolated samples, and the results were entirely reproducible. As expected, all the main clusters of peaks detected in A-LPS were also detected in the lipid A spectrum of *P. gingivalis* W50 total LPS, representing mono- and nonphosphorylated penta-acylated lipid A and mono- and nonphosphorylated tetra-acylated lipid A species. The clusters of peaks around *m/z* 1,376 in both lipid A species from A-LPS and total LPS from W50 (Fig. 4A and B) were viewed at a higher resolution (data not shown), and it was apparent that there was a series of ions (differing by approximately 2 Da) present in each case. Ions with the same *m/z* were present in both spectra but in various amounts. As a result, the *m/z* values shown within these clusters in Fig. 4 appear at

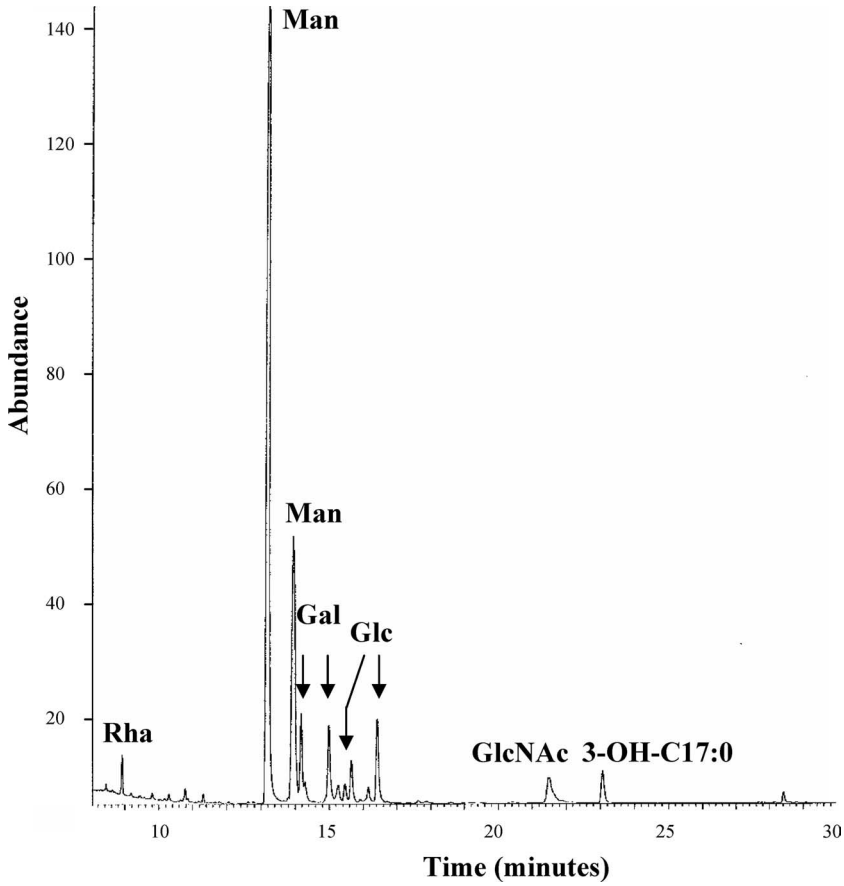

FIG. 3. Monosaccharide analysis of APS by methanolysis and GC-MS of *O*-TMS ethers. Lectin-purified APS was subjected to methanolysis (0.5 M methanolic HCl), followed by N-acetylation and conversion of methyl-glycosides to *O*-TMS ethers and GC-MS as described in the text. Multiple peaks for Man, Gal, and Glc are indicated. There is also a peak for 3-OH $C_{17:0}$.

slightly different *m*/*z* values in each sample, but this is simply a result of the envelope of ions present at low resolution being skewed because of the different proportions of individual species present in each spectrum. In addition, a cluster of peaks around *m*/*z* 1,772 was present in *P. gingivalis* W50, representing the diphosphorylated penta-acylated species (12, 13), and a minor cluster at *m*/*z* 1,280 was also present (Fig. 4B).

In the case of lipid A of LPS from the *P. gingivalis porR* mutant strain, a less heterogeneous spectrum than that of lipid A of LPS from *P. gingivalis* W50 was obtained. In particular, no signals for the nonphosphorylated penta-acylated and nonphosphorylated tetra-acylated species were detected (Fig. 4C). As the *porR* strain contains only lipid A derived from O-LPS, it appears that the two nonphosphorylated species (boxed in Fig. 4) may be unique to A-LPS. Hence, total lipid A from *P. gingivalis* W50 may represent a composite of different lipid A species derived from the two forms of LPS in this bacterium.

Biological activities of lipid A from *P. gingivalis* total LPS and A-LPS. *P. gingivalis* LPS has the capacity to elicit a variety of responses including cytokine production in human monocytes (6), and this led us to study the ability of lipid A from A-LPS to stimulate the proinflammatory cytokine production of, namely, IL-1α, IL-1β, IL-6, and IL-8 in human monocytes and compare it to the effects of lipid A from total LPS. Lipid A was used in the biological assays since it is more soluble than A-LPS, and the measurement of the endotoxin concentration was also more reliable.

Initially, we investigated the possible cytotoxic effects of *P. gingivalis* total lipid A and lipid A from A-LPS on MonoMac-6 cells in the range of 0.06 to 2.5 EU/ml. Cell viability was unaffected under all conditions, as shown by the levels of extracellularly released LDH, which were not significantly elevated compared to those of the unchallenged control (results not shown).

MonoMac-6 cells were stimulated with increasing concentrations of *P. gingivalis* lipid A from total LPS or lipid A from A-LPS (0.06 EU/ml to 2.5 EU/ml). Both forms of lipid A elicited IL-1α, IL-1β, IL-6, and IL-8 production by MonoMac-6 cells in a dose-dependent manner (Fig. 5). However, the cytokine-stimulating capacity of *P. gingivalis* lipid A from total LPS was clearly greater than that of lipid A from A-LPS, especially at 2.5 EU/ml. Compared to untreated cells, total lipid A increased IL-1α production by 104- ± 9-fold, whereas lipid A from A-LPS increased IL-1α production by 25.7- ± 1-fold (Fig. 5A). IL-1β production was enhanced by 120- ± 26-fold versus 16.6- ± 2-fold by total lipid A and lipid A from A-LPS, respectively (Fig. 5B). IL-6 was increased by 1,508- ± 18-fold by lipid A from total LPS, compared to lipid A from A-LPS, which increased IL-6 only by 290- ± 36-fold (Fig. 5C). IL-8 production was increased by 134- ± 1-fold versus 19- ±

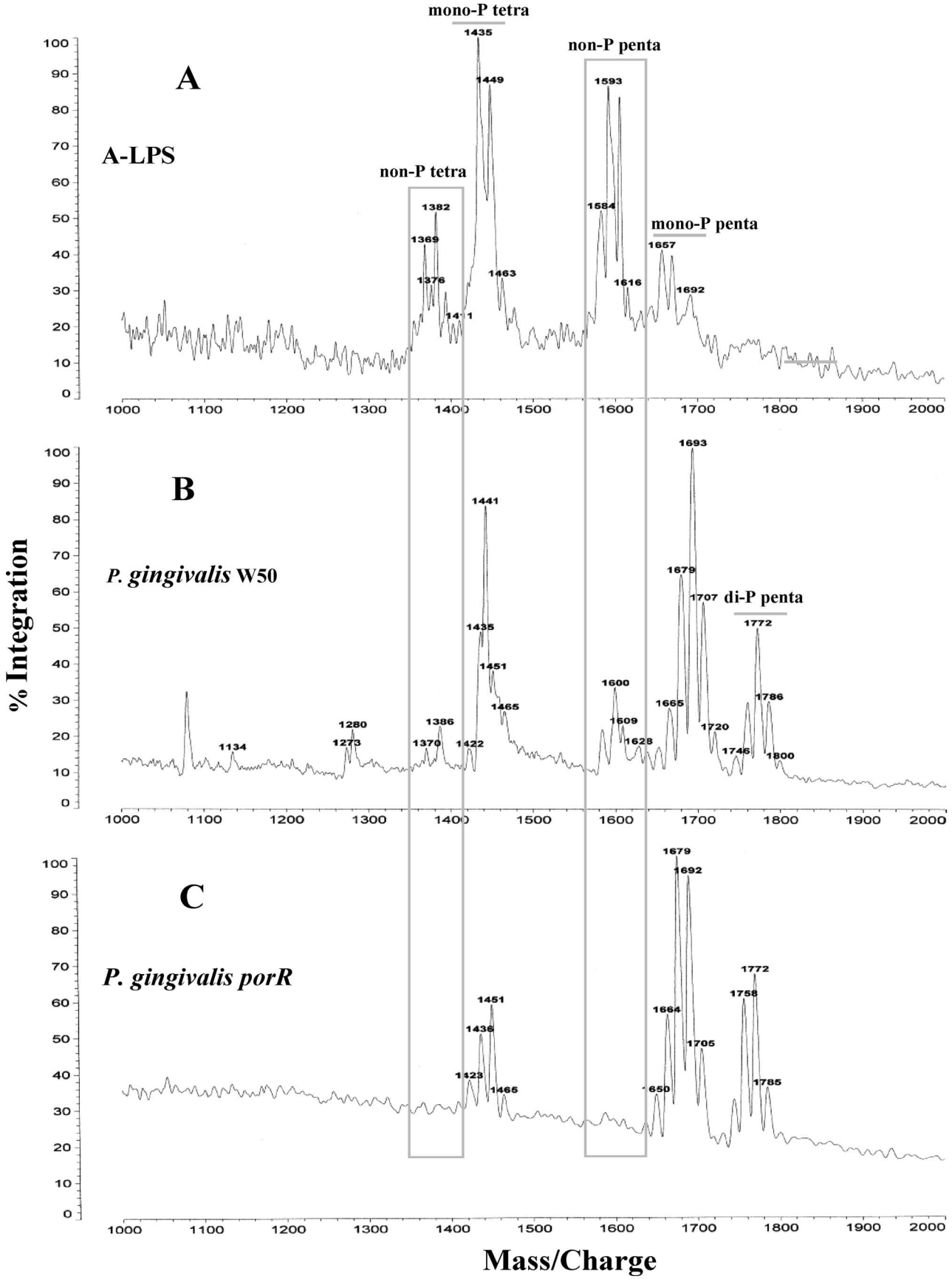

FIG. 4. MALDI-ToF MS of lipid A from LPS of *P. gingivalis* W50 and *porR* mutant strains. A-LPS (A), total LPS from *P. gingivalis* W50 (B), and LPS from the *P. gingivalis porR* mutant strain (C) were used to prepare lipid A as described in Materials and Methods. Lipid A was analyzed by MALDI-ToF MS in the negative-ion mode using Norharmane as the matrix.

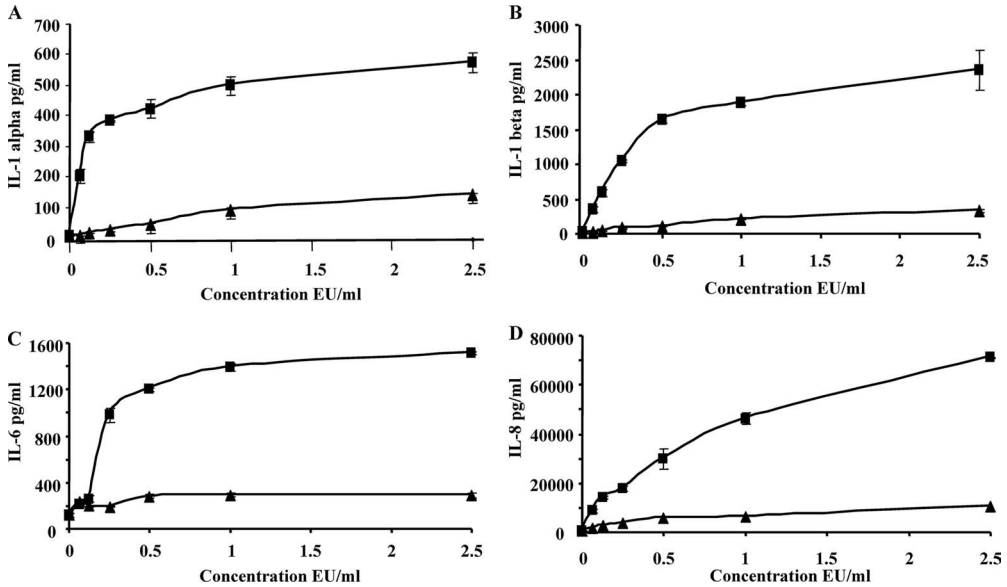

FIG. 5. Cytokine production by MonoMac-6 cells stimulated by lipid A from *P. gingivalis* total LPS and A-LPS. MonoMac-6 cells were plated at a density of 1×10^6 cells/ml in six-well dishes. Cells were exposed to either medium, lipid A from total LPS, or lipid A from A-LPS at the indicated concentrations for 6 h. The cells were then lysed, and cell-free supernatants were used to measure total levels of IL-1α (A), IL-1β (B), IL-6 (C), and IL-8 (D) by ELISA. Results are presented as means ± standard deviations of measurements done in triplicate. ■, lipid A from total LPS; ▲, lipid A from A-LPS.

1-fold by lipid A from total LPS and lipid A from A-LPS, respectively (Fig. 5D). These results strongly suggest that lipid A from A-LPS differs from lipid A from total LPS in its capacity to elicit cytokine production by human monocytes.

Identification of a putative O-antigen ligase at PG1051. In the next series of experiments, we sought to obtain independent evidence that A-LPS of *P. gingivalis* is ligated to a lipid A core and thus represents a second LPS in this bacterium. The final step in LPS assembly is catalyzed by the O-antigen ligase WaaL, which transfers preformed O antigen from an undecaprenyl lipid carrier onto the lipid A core at the periplasmic face of the cytoplasmic membrane. For other organisms, it was previously suggested that WaaL may have a relaxed specificity, allowing it to transfer O antigens of differing serotypes/structures onto the same lipid A core acceptor moiety (1, 17, 33). We therefore hypothesized that a WaaL in *P. gingivalis* may be able to catalyze the final step of both O-LPS and A-LPS biosynthesis through the transfer of O antigen and the phosphorylated branched mannan, respectively, onto a lipid A core. Using WaaL proteins from *E. coli*, *Salmonella enterica* serovar Typhimurium, *Klebsiella pneumoniae*, and *Vibrio cholerae*, we interrogated the *P. gingivalis* W83 genome (26) (http://cmr.tigr.org/tigr-scripts/CMR/GenomePage.cgi?database=gpg) for potential orthologues.

O-antigen ligases in different bacteria do not tend to display extensive sequence similarity. For example, WaaL proteins from *E. coli*, *Salmonella enterica* serovar Typhimurium, *Klebsiella pneumoniae*, and *Vibrio cholerae* display no significant sequence conservation. We identified PG1051 on the basis of extremely weak to marginal amino acid sequence similarity to this group of WaaL proteins. O-antigen ligases are integral membrane proteins usually with at least seven transmembrane domains followed by an O-antigen polymerase motif and a minimum of one transmembrane domain at the C terminus irrespective of the size of the protein. The C terminus of PG1051 possesses a motif (conserved domain architecture) corresponding to Wzy (O-antigen polymerase), which is indicative of a possible link to steps in LPS biosynthesis, and a Kyte and Doolittle hydrophobicity plot revealed an arrangement of putative transmembrane domains similar to that seen in WaaL proteins of other organisms. Thus, an isogenic mutant was generated via electrotransformation and allelic exchange.

Genomic organization at the PG1051 locus. PG1051 is the central gene of a locus that exhibits features of an operon (Fig. 6). The only proteins in the database with appreciable similarity to PG1050 (43% over 288 amino acids) are BF3443 from *Bacteroides fragilis* strain NCTC9343 and BF3641 from strain YCH46, which are both classified as putative lipoproteins. PG1052 has sequence similarity to MerR (70% over 110 amino acids), a component of the mercury resistance family of transcriptional regulators related to stress. PG1050 and PG1051 are separated by 41 bp, and PG1051 and PG1052 are 64 bp apart. As the direction of transcription is the same for all three genes, they could form part of a polycistronic message. Thus, although the intergenic sequences are sufficient to encode the transcription machinery for each gene, it was important to demonstrate that the knockout of PG1051 had no polar effects on the transcription of neighboring genes. Reverse transcription-PCR showed the absence of polar effects (Fig. 6C). PG1050 and PG1052 are expressed in parent strain *P. gingivalis* W50 and in mutant strain PG1051-KO, confirming the absence of polar effects on both upstream and downstream genes.

Properties of mutant strain *P. gingivalis* PG1051-KO. We first examined whether the inactivation of the putative ligase at PG1051 had abolished the addition of the O antigen to the lipid A core in this mutant. LPS was isolated from *P. gingivalis*

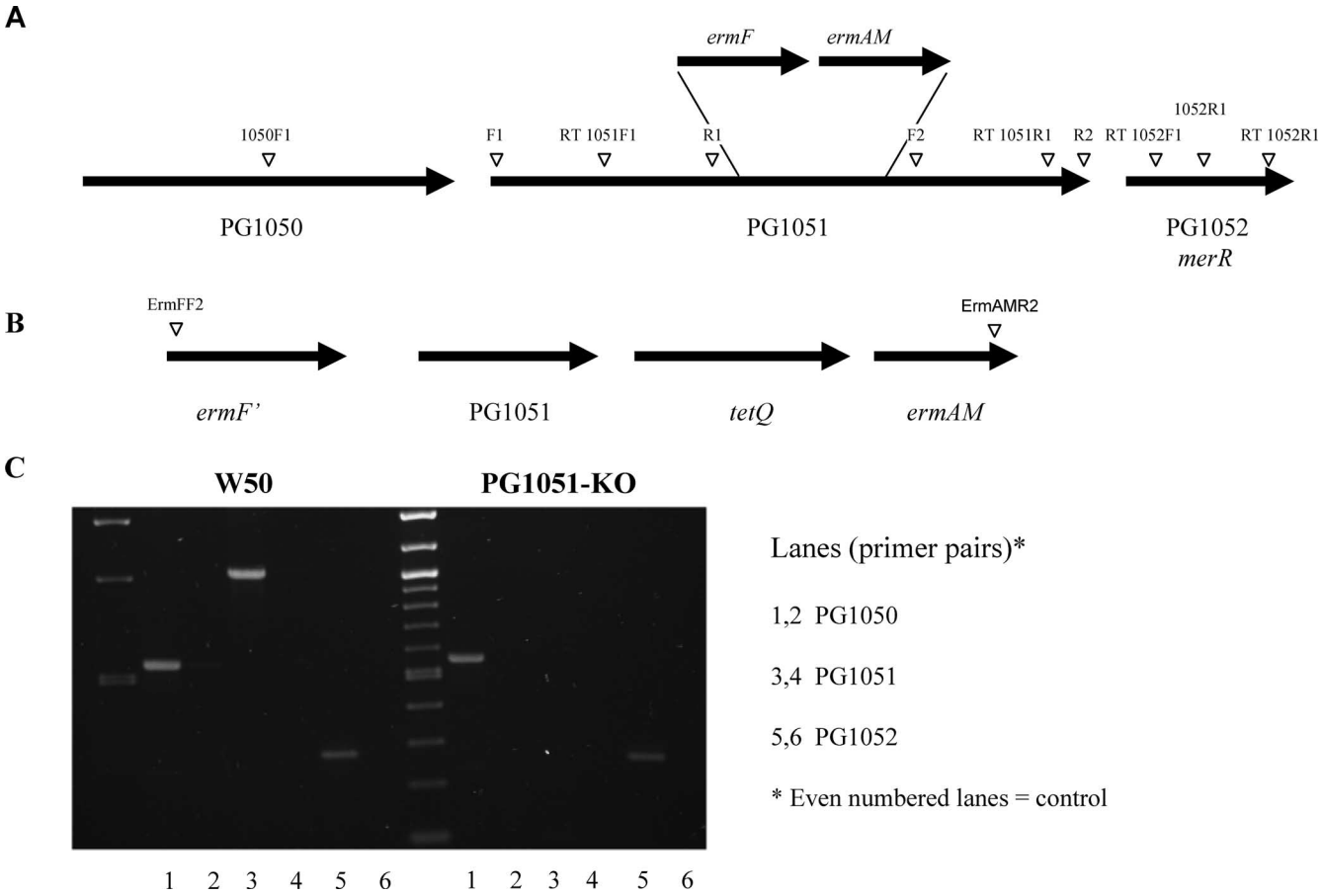

FIG. 6. Genetic analysis of the *P. gingivalis* "ligase" locus and expression by reverse transcription-PCR. (A) Diagrammatic representation of the genomic locus of PG1051. The position of the *erm* cassette used to generate the isogenic mutant *P. gingivalis* PG1051-KO and oligonucleotide primers are indicated. (B) Complementation of *P. gingivalis* PG1051. The genetic structure of the new locus and primer pair ErmFF2 and ErmAMR2, used for screening, are indicated. (C) Expression of PG1051. The primer pair for each gene includes a control (right-hand lane) to exclude possible contamination of the RNA sample by chromosomal DNA. Reverse transcriptase (RT) was not included in the controls.

W50 and PG1051-KO using the phenol-guanidine thiocyanate method (in which LPS is extracted into the aqueous phase after the addition of chloroform) and subjected to SDS-urea-PAGE using a bilayer stacking gel (19). No laddering pattern was obtained from the PG1051-KO LPS sample (data not shown), whereas LPS from *P. gingivalis* W50 shows the characteristic repeating-unit profile in this gel electrophoresis system (Fig. 7). The absence of silver staining material close to the running front of the PG1051-KO mutant suggested that the phenol-guanidine thiocyanate method may have failed to extract LPS or lipid A core from this strain since the method relies on the polar properties of the O antigen. We therefore purified LPS from strain PG1051-KO according to a method described previously by Westphal and Jann (40), followed by digestion of the extract with DNase, RNase, and protease. In this instance, there were two silver-stained bands, one at the running front and a second band that may represent LPS containing one repeating unit running just above the running front (Fig. 7).

Further evidence that the inactivation of PG1051 in *P. gingivalis* W50 may have compromised the LPS structure was observed during growth on blood agar plates, which revealed colonies with significantly increased zones and rates of hemolysis (Fig. 8A) after 4 days of growth. The perturbation of outer membrane structure leading to a "leaky" membrane, which releases periplasmic proteins into the medium, is frequently associated with changes in the composition of LPS, particularly the heptose region of the core OS, the so-called deep-rough phenotype (16). Interestingly, the inactivation of PG1051 also led to a loss of the characteristic black pigmentation of the organism on these plates. In liquid culture in BHI broth, the growth rate and cell yield of the mutant strain were comparable to those of parent strain W50 up to 48 h (Fig. 8B), although the cells appeared to adhere to each other, resulting in rapid sedimentation. However, between 48 h and 144 h, there was a rapid decline in the cell density of the PG1051-KO mutant strain, indicating increased cell lysis (Fig. 8B). This may be due to a defect in the cell wall of strain PG1051-KO due to the absence of an essential structural component, as was observed for a *P. gingivalis porR* mutant strain (30).

Figures 8C and D show electron micrographs of *P. gingivalis* W50 and PG1051-KO, respectively, from liquid cultures grown for 24 h, which demonstrate a reduction in the electron-dense surface layer of cells from mutant strain PG1051-KO.

Immunochemical analysis on Western blots using MAb 1B5

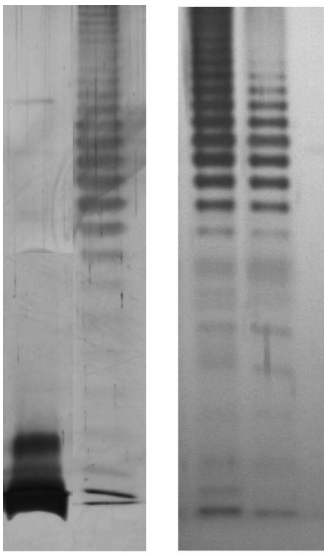

FIG. 7. SDS-urea-PAGE of LPS from *P. gingivalis* W50, PG1051-KO, and PG1051$^+$ strains. (A) SDS-urea-PAGE of LPS prepared using the phenol-guanidine isothiocyanate method. (B) SDS-PAGE of LPS prepared from a *P. gingivalis* PG1051-KO strain according to a method described previously by Darveau and Hancock (40). Lanes: 1, PG1051-KO LPS; 2 and 3, W50 LPS; 4, PG1051$^+$ LPS.

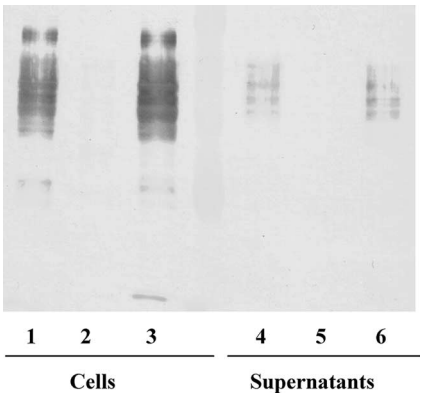

FIG. 9. Immunochemical analysis of *P. gingivalis* W50, PG1051-KO, and PG1051$^+$ strains. *P. gingivalis* strains were grown in BHI broth for 48 h. Proteins in culture supernatants were precipitated with 2 volumes of acetone at −20°C and separated by centrifugation. Whole cells and protein precipitates were treated with leupeptin to inhibit Arg-gingipains, treated with SDS sample buffer, subjected to SDS-PAGE and Western blotting, and probed with MAb 1B5. Lanes: 1 and 4, W50; 2 and 5, PG1051-KO; 3 and 6, PG1051$^+$.

showed that mutant strain PG1051-KO failed to cross-react with this antibody, indicating the absence of A-LPS in this strain (Fig. 9). Hence, the inactivation of PG1051 results in not only the lack of a detectable O-antigen repeating unit attached to O-LPS but also the abolition of detectable APS attached to A-LPS in this organism.

The original parental genotype and phenotype were restored in complemented strain PG1051$^+$. Black pigmentation; reduced hemolysis (Fig. 8A), growth rate, and cell yields for 144 h (Fig. 8B); and cross-reactivity to MAb 1B5 (Fig. 9) were all identical to those of parent strain *P. gingivalis* W50. Similarly, SDS-urea-PAGE of LPS of PG1051$^+$ showed the char-

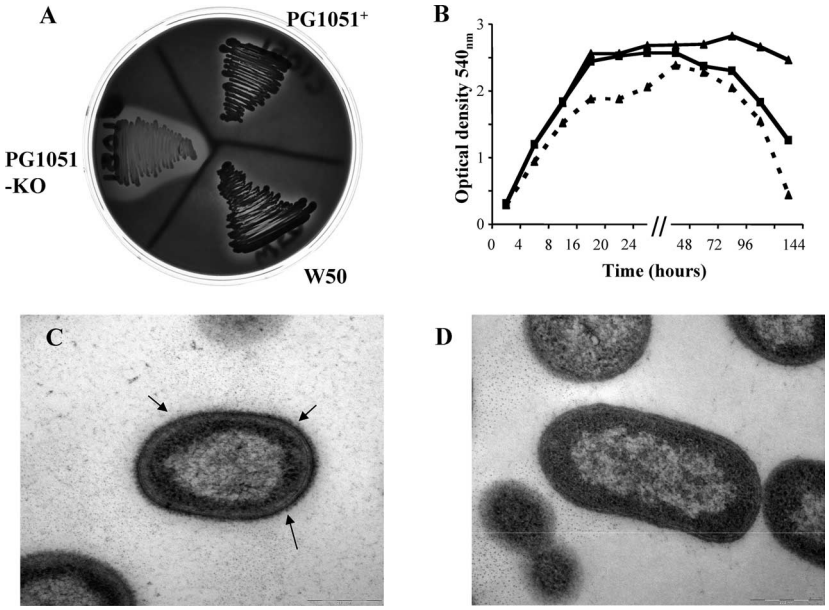

FIG. 8. Hemolysis, growth rates, and transmission electron microscopy of *P. gingivalis* W50, PG1051-KO, and PG1051$^+$ strains. (A) *P. gingivalis* W50, PG1051-KO, and PG1051$^+$ strains were grown anaerobically on a blood agar plate for 4 days. (B) Strains were grown in an anaerobic cabinet in BHI broth supplemented with hemin. Samples were withdrawn at different time points, and the optical density was measured at 540 nm for 6 days. ▲—▲, *P. gingivalis* W50; (▲—▲), PG1051-KO; ■, PG1051$^+$. (C and D) Electron micrographs of *P. gingivalis* W50 (C) and PG1051-KO mutant strains (D) grown in liquid culture (24 h). Arrows indicate the electron-dense region surrounding *P. gingivalis* W50 cells.

acteristic laddering pattern obtained with the parent strain (Fig. 7).

DISCUSSION

The results described above show that *P. gingivalis* contains two LPS macromolecules, an O-LPS containing the O antigen attached to the lipid A core and an A-LPS in which the phosphorylated branched mannan repeating unit is attached to the lipid A core. However, we have not been able to purify large quantities of A-LPS in order to determine the structure of the core OS and attachment point of the APS repeating units.

The presence of more than one LPS species in a bacterium is not unprecedented. Some bacteria contain multiple lipid A core-linked polymers. In *E. coli*, the lipid A core can act as an anchor for O antigen for one form of the enterobacterial common antigen (ECA) polymer (21), a subset of group 1 capsular K antigens (42), and a colanic acid (M antigen) repeating unit (25). In *E. coli* strains with group 1 (A and B) capsules, K antigen is expressed on the cell surface in two forms, one of which, K_{LPS}, comprises low-molecular-weight K-antigen OS linked to the lipid A core. In contrast, the high-molecular-weight capsular antigen is not linked to the lipid A core (24). A highly mucoid strain of *E. coli* ligates colanic acid repeating units to core OS, forming the novel LPS glycoform called M LPS (25). The attachment point was identified as being O-7 of L-*glycero*-D-*manno*-heptose of the outer core OS, which is the same position used for O-antigen ligation. *Pseudomonas aeruginosa* expresses two lipid A core-linked polymers: a conserved polyrhamnose homopolymer known as A-band LPS, which is analogous to lipid A core-linked ECA, and a serotype-specific O antigen known as B-band LPS (35). This shows that the lipid A core is a versatile anchor for the presentation of cell surface PS.

We therefore investigated whether the final step in the synthesis of LPS, i.e., the ligation of O antigen/phosphorylated branched mannan to the lipid A core, was catalyzed by the same enzyme. LPS biosynthesis in gram-negative bacteria involves a large number of enzymes synthesized by more than 40 genes (16, 17, 43). The core OS is assembled on preformed lipid A by the sequential addition of sugar components by glycosyl transferases, whereas the O antigen (if it is not a homopolymer) is usually assembled as repeating units on undecaprenylpyrophosphate (Und-P-P) on the cytosolic side of the cytoplasmic membrane (41, 43). Following their assembly, individual Und-P-P-linked O-antigen subunits are translocated across the cytoplasmic membrane, where they are polymerized by the successive addition of the reducing end of the growing O-antigen chain to the nonreducing end of the Und-P-P-linked repeating subunit. This is referred to as the *wzy* (polymerase)-dependent pathway and is thought to occur in the majority of O antigens (14). The ligation of the polymerized O antigen onto the lipid A core acceptor molecule with the release of Und-P-P is the final step in the biosynthesis of LPS and occurs on the periplasmic side of the membrane (33). WaaL (O-antigen ligase) acts on the periplasmic face of the cytoplasmic membrane and is the only gene product that appears to be necessary to ligate newly synthesized polymeric O antigen to the lipid A core (16). All WaaL proteins are predicted to be integral membrane proteins with eight or more membrane-spanning domains and a C-terminal domain (Wzy [O-antigen polymerase]), indicating a probable link with the regulation of chain length of O-antigen biosynthesis. Ligases show no specificity for the structure of the ligated PS, probably because the PS is presented for ligation in a common Und-P-P-linked form. These enzymes can efficiently ligate high-molecular-weight polymers or low-molecular-weight OSs to the lipid A core.

In *P. aeruginosa*, LPS from a *waaL* knockout mutant strain is devoid of B-band O-PS, semirough LPS, and A-band O-PS (1). Complementation of the *waaL* mutant strain with a plasmid containing *waaL* restored the production of both A-band and B-band O antigens as well as semirough LPS, indicating that the same WaaL is required for the attachment of O-antigen PS to the lipid A core. Mutations of *waaL* in *P. aeruginosa* strains PA01 and PA14 could be complemented with *waaL* from either strain to restore the production of wild-type LPS (1). *E. coli* WaaL is required for the attachment of type 1 capsular PS, one form of ECA, and the attachment of colanic acid repeating units (25) to the same lipid A core. These studies confirm the broad specificity of ligase(s) for ligating undecaprenolpyrophosphate-linked O antigens to the lipid A core.

The inactivation of PG1051 in *P. gingivalis* leads to the loss of intact O-LPS and A-LPS, indicating that the transfer of O-PS and phosphorylated branched mannan to the lipid A core is PG1051 dependent, and suggests that the product is a WaaL, glycan ligase, with relaxed specificity in common with other known ligases (1). Power et al. (31) previously described an O-antigen ligase mutant (*pglL*) in *Neisseria meningitidis* that showed no change in LPS phenotype but showed a loss of pilin glycosylation, suggesting that this system may have evolved out of the O-antigen biosynthesis pathway, and that has become specific for OS transfer to a Ser residue on pilin. Given that epitopes derived from APS are also attached to the Arg-gingipain protease family of *P. gingivalis* (10, 30), it is possible that there may be a link between the PG1051 ligase and glycosylation reactions in this organism, and this will form the subject of future studies.

It was initially thought that lipid A of LPS from *P. gingivalis* possessed limited structural heterogeneity comprising only a triacylated monophosphorylated form with a negative-ion mass of *m/z* 1,195 (28). However, Kumada et al. (22) later showed that *P. gingivalis* lipid A was present in several structural isoforms including tetra- and penta-acylated monophosphorylated lipid A's with molecular mass ions of *m/z* 1,435, *m/z* 1,449, and *m/z* 1,690. These variations were thought to be due to differences in the strains of *P. gingivalis*, growth conditions, and procedures used for the isolation of LPS. However, LPS purified from several laboratory strains as well as clinical isolates contained multiple lipid A species (12). Different techniques used to extract LPS, such as phenol-guanidine thiocyanate (44) or cold $MgCl_2$ (11), have still yielded LPS with multiple lipid A moieties, suggesting that heterogeneity might not be a function of strain differences or extraction procedures alone but could also be due to environmental factors. Thus, lipid A of *P. gingivalis* is now recognized as a moiety in which modification can result in multiple forms where each one has a potentially distinct effect on the innate host response (34).

Two unusual lipid A species were detected in A-LPS, namely, a nonphosphorylated penta-acylated form and a nonphosphorylated tetra-acylated form. These were also present in

the total lipid A extract of LPS from whole *P. gingivalis* W50 cells but were absent in lipid A from the LPS of a *porR* mutant strain that lacks A-LPS (30) and synthesizes only O-LPS. Hence, these preliminary findings suggest that there may be subtle differences between the lipid A species of O-LPS and A-LPS, which may be reflected in the potencies of their respective interactions with the pattern recognition systems of the host. Future investigations will therefore explore the relative contributions of these two macromolecules to the net inflammatory potential of *P. gingivalis* and how potential variations in their proportions may influence the pathogenic phenotype.

Reife et al. (34) showed that the heterogeneity in the lipid A structures of *P. gingivalis* ATCC 33277 causes distinct and opposing effects on the innate host response. Several studies suggested previously that *P. gingivalis* LPS can act as a Toll-like receptor 4 (TLR4) agonist and antagonist (8, 39, 45). For example, Reife et al. (34) showed previously that penta-acylated monophosphoryl lipid A structures act as agonists for E-selectin expression in human umbilical cord vein endothelial cells, whereas tetra-acylated monophosphoryl structures do not and are in fact potent antagonists for E-selectin expression. Darveau et al. (12) previously described the ability of a *P. gingivalis* LPS preparation enriched in tetra-acylated monophosphoryl lipid A structure to signal through both TLR2 and TLR4 receptors. Those studies indicate that minor changes in lipid A structures can significantly modify the innate host response. We investigated the ability of lipid A from A-LPS and total LPS of *P. gingivalis* W50 to induce the production of IL-1α, IL-1β, IL-6, and IL-8 in human monocytes. Lipid A from A-LPS was able to induce cytokine production by human monocytes, although it is a much weaker inducer than lipid A from total LPS. Since there are variations not only in the fatty acid compositions but also in the degrees of phosphorylation of bis-GlcNAc in lipid A from A-LPS and O-LPS (Fig. 5), the differences observed in the experiments with human monocytes could be attributed to these structural differences.

We therefore conclude that *P. gingivalis* synthesizes two distinct LPS macromolecules and that the final step in the assembly of both macromolecules is catalyzed by a relaxed-specificity ligase, which is able to attach either a branched phosphorylated mannan or the previously recognized tetrasaccharide repeating unit to a lipid A core. Given that differences exist in the phosphorylation statuses of the lipid A's of A-LPS and O-LPS, it is possible that they may have different properties with respect to their interactions with the immune system of the colonized host. The processes that govern the relative proportions of these two macromolecules and their physiological relevance are under investigation.

ACKNOWLEDGMENTS

This investigation was supported by Medical Research Council (United Kingdom) grant no. G0501478 and the Research Advisory Board of the Barts and The London Charity, grant reference no. RAB06/PJ/14.

REFERENCES

1. **Abeyrathne, P. D., C. Daniels, K. K. Poon, M. J. Matewish, and J. S. Lam.** 2005. Functional characterization of WaaL, a ligase associated with linking O-antigen polysaccharide to the core of *Pseudomonas aeruginosa* lipopolysaccharide. J. Bacteriol. **187:**3002–3012.
2. **Aduse-Opoku, J., J. Muir, J. M. Slaney, M. Rangarajan, and M. A. Curtis.** 1995. Characterization, genetic analysis, and expression of a protease antigen (PrpRI) of *Porphyromonas gingivalis* W50. Infect. Immun. **63:**4744–4754.
3. **Aduse-Opoku, J., J. M. Slaney, A. Hashim, A. Gallagher, R. P. Gallagher, M. Rangarajan, K. Boutaga, M. L. Laine, A. J. van Winkelhoff, and M. A. Curtis.** 2006. Identification and characterization of the capsular polysaccharide (K-antigen) locus of *Porphyromonas gingivalis*. Infect. Immun. **74:**449–460.
4. **Al Qutub, M. N., P. H. Braham, L. M. Karimi-Naser, X. Liu, C. A. Genco, and R. P. Darveau.** 2006. Hemin-dependent modulation of the lipid A structure of *Porphyromonas gingivalis* lipopolysaccharide. Infect. Immun. **74:**4474–4485.
5. **Altman, E., M. B. Perry, and J. R. Brisson.** 1989. Structure of the lipopolysaccharide antigenic O-chain produced by *Actinobacillus pleuropneumoniae* serotype 4 (ATCC 33 378). Carbohydr. Res. **191:**295–303.
6. **Bostanci, N., R. Allaker, U. Johansson, M. Rangarajan, M. A. Curtis, F. J. Hughes, and I. J. McKay.** 2007. Interleukin-1alpha stimulation in monocytes by periodontal bacteria: antagonistic effects of Porphyromonas gingivalis. Oral Microbiol. Immunol. **22:**52–60.
7. **Bury, C. L.** 2004. Analysis of multiple product formation from a single gene from the anaerobic bacterium *Porphyromonas gingivalis*. Ph.D. dissertation. University of London, London, United Kingdom.
8. **Coats, S. R., R. A. Reife, B. W. Bainbridge, T. T. Pham, and R. P. Darveau.** 2003. *Porphyromonas gingivalis* lipopolysaccharide antagonizes *Escherichia coli* lipopolysaccharide at Toll-like receptor 4 in human endothelial cells. Infect. Immun. **71:**6799–6807.
9. **Curtis, M. A., J. Aduse-Opoku, and M. Rangarajan.** 2001. Cysteine proteases of *Porphyromonas gingivalis*. Crit. Rev. Oral Biol. Med. **12:**192–216.
10. **Curtis, M. A., A. Thickett, J. M. Slaney, M. Rangarajan, J. Aduse-Opoku, P. Shepherd, N. Paramonov, and E. F. Hounsell.** 1999. Variable carbohydrate modifications to the catalytic chains of the RgpA and RgpB proteases of *Porphyromonas gingivalis* W50. Infect. Immun. **67:**3816–3823.
11. **Darveau, R. P., and R. E. Hancock.** 1983. Procedure for isolation of bacterial lipopolysaccharides from both smooth and rough *Pseudomonas aeruginosa* and *Salmonella typhimurium* strains. J. Bacteriol. **155:**831–838.
12. **Darveau, R. P., T. T. Pham, K. Lemley, R. A. Reife, B. W. Bainbridge, S. R. Coats, W. N. Howald, S. S. Way, and A. M. Hajjar.** 2004. *Porphyromonas gingivalis* lipopolysaccharide contains multiple lipid A species that functionally interact with both Toll-like receptors 2 and 4. Infect. Immun. **72:**5041–5051.
13. **Dixon, D. R., and R. P. Darveau.** 2005. Lipopolysaccharide heterogeneity: innate host responses to bacterial modification of lipid A structure. J. Dent. Res. **84:**584–595.
14. **Feldman, M. F., C. L. Marolda, M. A. Monteiro, M. B. Perry, A. J. Parodi, and M. A. Valvano.** 1999. The activity of a putative polyisoprenol-linked sugar translocase (Wzx) involved in *Escherichia coli* O antigen assembly is independent of the chemical structure of the O repeat. J. Biol. Chem. **274:**35129–35138.
15. **Fletcher, H. M., H. A. Schenkein, R. M. Morgan, K. A. Bailey, C. R. Berry, and F. L. Macrina.** 1995. Virulence of a *Porphyromonas gingivalis* W83 mutant defective in the *prtH* gene. Infect. Immun. **63:**1521–1528.
16. **Heinrichs, D. E., J. A. Yethon, and C. Whitfield.** 1998. Molecular basis for structural diversity in the core regions of the lipopolysaccharides of *Escherichia coli* and *Salmonella enterica*. Mol. Microbiol. **30:**221–232.
17. **Heinrichs, D. E., M. A. Monteiro, M. B. Perry, and C. Whitfield.** 1998. The assembly system for the lipopolysaccharide R2 core-type of *Escherichia coli* is a hybrid of those found in *Escherichia coli* K-12 and *Salmonella enterica*. Structure and function of the R2 WaaK and WaaL homologs. J. Biol. Chem. **273:**8849–8859.
18. **Herrero, M., V. De Lorenzo, and K. N. Timmis.** 1990. Transposon vectors containing non-antibiotic resistance selection markers for cloning and stable chromosomal insertion of foreign genes in gram-negative bacteria. J. Bacteriol. **172:**6557–6567.
19. **Inzana, T. J., and M. A. Apicella.** 1999. Use of a bilayer stacking gel to improve resolution of lipopolysaccharides and lipooligosaccharides in polyacrylamide gels. Electrophoresis **20:**462–465.
20. **Kakehi, K., and S. Honda.** 1989. Analysis of carbohydrates by GLC and MS. CRC Press, Boca Raton, FL.
21. **Kuhn, H. M., U. Meier-Dieter, and H. Mayer.** 1988. ECA, the enterobacterial common antigen. FEMS Microbiol. Rev. **4:**195–222.
22. **Kumada, H., Y. Haishima, T. Umemoto, and K. Tanamoto.** 1995. Structural study on the free lipid A isolated from lipopolysaccharide of *Porphyromonas gingivalis*. J. Bacteriol. **177:**2098–2106.
23. **Laemmli, U. K.** 1970. Cleavage of structural proteins during the assembly of the head of bacteriophage T4. Nature **227:**680–685.
24. **MacLachlan, P. R., W. J. Keenleyside, C. Dodgson, and C. Whitfield.** 1993. Formation of the K30 (group I) capsule in *Escherichia coli* O9:K30 does not require attachment to lipopolysaccharide lipid A-core. J. Bacteriol. **175:**7515–7522.
25. **Meredith, T. C., U. Mamat, Z. Kaczynski, B. Lindner, O. Holst, and R. W. Woodard.** 2007. Modification of lipopolysaccharide with colanic acid (M-antigen) repeats in Escherichia coli. J. Biol. Chem. **282:**7790–7798.

26. **Nelson, K. E., R. D. Fleischmann, R. T. DeBoy, I. T. Paulsen, D. E. Fouts, J. A. Eisen, S. C. Daugherty, R. J. Dodson, A. S. Durkin, M. Gwinn, D. H. Haft, J. F. Kolonay, W. C. Nelson, T. Mason, L. Tallon, J. Gray, D. Granger, H. Tettelin, H. Dong, J. L. Galvin, M. J. Duncan, F. E. Dewhirst, and C. M. Fraser.** 2003. Complete genome sequence of the oral pathogenic bacterium *Porphyromonas gingivalis* strain W83. J. Bacteriol. **185:**5591–5601.
27. **Ogawa, T., Y. Kusumoto, S. Hamada, J. R. McGhee, and H. Kiyono.** 1990. *Bacteroides gingivalis*-specific serum IgG and IgA subclass antibodies in periodontal diseases. Clin. Exp. Immunol. **82:**318–325.
28. **Ogawa, T.** 1993. Chemical structure of lipid A from *Porphyromonas* (*Bacteroides*) *gingivalis* lipopolysaccharide. FEBS Lett. **332:**197–201.
29. **Paramonov, N., D. Bailey, M. Rangarajan, A. Hashim, G. Kelly, M. A. Curtis, and E. F. Hounsell.** 2001. Structural analysis of the polysaccharide from the lipopolysaccharide of *Porphyromonas gingivalis* strain W50. Eur. J. Biochem. **268:**4698–4707.
30. **Paramonov, N., M. Rangarajan, A. Hashim, A. Gallagher, J. Aduse-Opoku, J. M. Slaney, E. Hounsell, and M. A. Curtis.** 2005. Structural analysis of a novel anionic polysaccharide from *Porphyromonas gingivalis* strain W50 related to Arg-gingipain glycans. Mol. Microbiol. **58:**847–863.
31. **Power, P. M., K. L. Seib, and M. P. Jennings.** 2006. Pilin glycosylation in *Neisseria meningitidis* occurs by a similar pathway to wzy-dependent O-antigen biosynthesis in *Escherichia coli*. Biochem. Biophys. Res. Commun. **347:**904–908.
32. **Que-Gewirth, N. L., A. A. Ribeiro, S. R. Kalb, R. J. Cotter, D. M. Bulach, B. Adler, I. S. Girons, C. Werts, and C. R. Raetz.** 2004. A methylated phosphate group and four amide-linked acyl chains in Leptospira interrogans lipid A. The membrane anchor of an unusual lipopolysaccharide that activates TLR2. J. Biol. Chem. **279:**25420–25429.
33. **Raetz, C. R., and C. Whitfield.** 2002. Lipopolysaccharide endotoxins. Annu. Rev. Biochem. **71:**635–700.
34. **Reife, R. A., S. R. Coats, M. Al Qutub, D. M. Dixon, P. A. Braham, R. J. Billharz, W. N. Howald, and R. P. Darveau.** 2006. *Porphyromonas gingivalis* lipopolysaccharide lipid A heterogeneity: differential activities of tetra- and penta-acylated lipid A structures on E-selectin expression and TLR4 recognition. Cell. Microbiol. **8:**857–868.
35. **Rocchetta, H. L., L. L. Burrows, and J. S. Lam.** 1999. Genetics of O-antigen biosynthesis in *Pseudomonas aeruginosa*. Microbiol. Mol. Biol. Rev. **63:**523–553.
36. **Shoji, M., D. B. Ratnayake, Y. Shi, T. Kadowaki, K. Yamamoto, F. Yoshimura, A. Akamine, M. A. Curtis, and K. Nakayama.** 2002. Construction and characterization of a nonpigmented mutant of *Porphyromonas gingivalis*: cell surface polysaccharide as an anchorage for gingipains. Microbiology **148:**1183–1191.
37. **Slaney, J. M., A. Gallagher, J. Aduse-Opoku, K. Pell, and M. A. Curtis.** 2006. Mechanisms of resistance of *Porphyromonas gingivalis* to killing by serum complement. Infect. Immun. **74:**5352–5361.
38. **Slaney, J. M., M. Rangarajan, J. Aduse-Opoku, S. Fawell, I. Darby, D. Kinane, and M. A. Curtis.** 2002. Recognition of the carbohydrate modifications to the RgpA protease of *Porphyromonas gingivalis* by periodontal patient serum IgG. J. Periodont. Res. **37:**215–222.
39. **Tabeta, K., K. Yamazaki, S. Akashi, K. Miyake, H. Kumada, T. Umemoto, and H. Yoshie.** 2000. Toll-like receptors confer responsiveness to lipopolysaccharide from *Porphyromonas gingivalis* in human gingival fibroblasts. Infect. Immun. **68:**3731–3735.
40. **Westphal, O., and K. Jann.** 1965. Methods in carbohydrate chemistry. Academic Press, New York, NY.
41. **Whitfield, C.** 1995. Biosynthesis of lipopolysaccharide O antigens. Trends Microbiol. **3:**178–185.
42. **Whitfield, C., and I. S. Roberts.** 1999. Structure, assembly and regulation of expression of capsules in *Escherichia coli*. Mol. Microbiol. **31:**1307–1319.
43. **Whitfield, C., and M. A. Valvano.** 1993. Biosynthesis and expression of cell-surface polysaccharides in gram-negative bacteria. Adv. Microb. Physiol. **35:**135–246.
44. **Yi, E. C., and M. Hackett.** 2000. Rapid isolation method for lipopolysaccharide and lipid A from gram-negative bacteria. Analyst **125:**651–656.
45. **Yoshimura, A., T. Kaneko, Y. Kato, D. T. Golenbock, and Y. Hara.** 2002. Lipopolysaccharides from periodontopathic bacteria *Porphyromonas gingivalis* and *Capnocytophaga ochracea* are antagonists for human Toll-like receptor 4. Infect. Immun. **70:**218–225.